

Orbital Debris

Quarterly News

Volume 28, Issue 2
April 2024

Inside...

Evolution of the
Cosmos 1408
Breakup Cloud 2

Modeling the Small
Debris Population
in ORDEM 4

Meeting Report 7

Upcoming
Meetings 7

Plot 8

Space Missions 9

Satellite
Box Score 10

2024 UN COPUOS STSC Session

The 61st session of the Scientific and Technical Subcommittee (STSC) of the United Nations' (UN) Committee on the Peaceful Uses of Outer Space (COPUOS) took place at the Vienna International Center in Vienna, Austria, from 28 January to 05 February. Under Agenda Item 6 ("Space Debris"), more than 20 COPUOS STSC Member States delivered statements expressing concerns for the growing threat from orbital debris and emphasizing the need to implement orbital debris mitigation best practices, such as the UN COPUOS Space Debris Mitigation Guidelines and the Inter-Agency Space Debris Coordination Committee (IADC) Space Debris Mitigation Guidelines to address the orbital debris problem. Several technical presentations on orbital debris were provided under the same agenda item, including:

- "2023 Space Debris Activities in France: Highlights"
- "2023 Space Debris Activities and Status in Republic of Korea"
- "An update on UKSA's Active Debris Removal Activities"
- "ASI activities on Space Debris"
- "ESA's zero debris approach"
- "IADC activities for 2023"
- "U.S. Space Debris Environment and Activity Updates"

These and other STSC presentations are available on the COPUOS website at <https://www.unoosa.org/oosa/en/ourwork/copuos/stsc/technical-presentations.html>.

The European Space Policy Institute with co-sponsorship from the United Kingdom Space Agency, also hosted an evening side event during STSC to celebrate the 30th anniversary of the IADC. The event began with an overview of the IADC followed by a panel with representatives from Germany, India, the United Kingdom, and the U.S. Panel discussions focused on promoting the IADC Space Debris Mitigation Guidelines and addressing several key orbital debris challenges facing the international community. Close to 100 participants from STSC Member States attended this very successful side event. ♦



The Vienna International Centre, home to the United Nations headquarters in Vienna. Credit: NASA ODPO



A publication of the
NASA Orbital Debris
Program Office (ODPO)

PROJECT REVIEW

Evolution of the Cosmos 1408 Breakup Cloud: A Two-Year Status

A. MANIS, M. MATNEY, AND P. ANZ-MEADOR

Soon after the direct-ascent antisatellite test (ASAT) against Cosmos 1408 on 15 November 2021 by the Russian Federation, the NASA Orbital Debris Program Office (ODPO) released a new version of the Orbital Debris Engineering Model (ORDEM), version 3.2, using analysis of special radar measurements to incorporate fragments from the breakup (ODQN vol. 26, issue 1, March 2022,

pp. 1-5). Data available at that time from the Goldstone Orbital Debris Radar, the Haystack Ultrawideband Satellite Imaging Radar (HUSIR), and the Space Fence indicated the modeled breakup using the NASA Standard Satellite Breakup Model (SSBM) matched radar measurements very well. The subsequent 2 years of statistical radar data collections by HUSIR on sub-centimeter-sized debris, as well as continued cataloging of fragments greater than approximately 10 cm, have allowed regular assessments of the state and evolution of the Cosmos 1408 breakup fragments. In particular, the debris cloud appears to be dragging out faster than originally estimated due to solar flux activity increasing at a faster rate and reaching higher levels than the original Solar Cycle 25 prediction [1]. This project review highlights the latest available data on the Cosmos 1408 breakup cloud from HUSIR and the Space Surveillance Network (SSN), as well as comparisons between the initial predictions used in ORDEM 3.2 development and new analysis using the recorded solar flux values for the 2 years following the breakup.

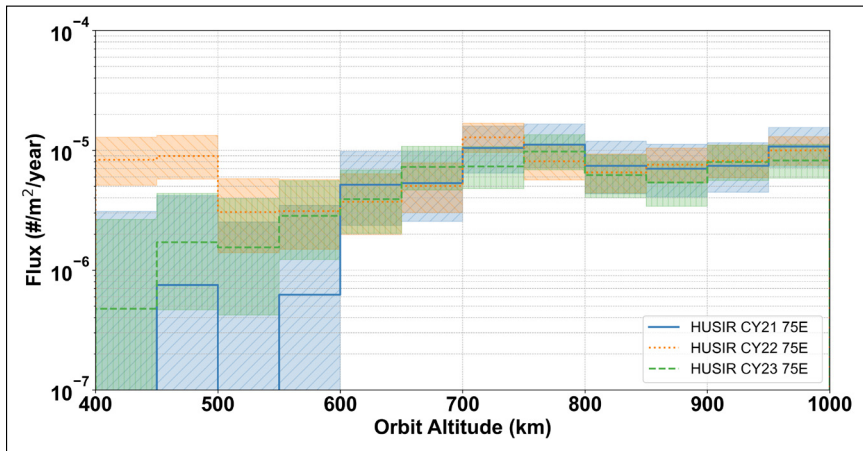


Figure 1. Debris surface area flux as a function of altitude from HUSIR CY 2021, CY 2022, and CY 2023, limited to objects with sizes 7.2 mm and larger, inclinations from 72° to 94°, and altitudes less than 1000 km. Shaded regions represent the 2σ Poisson confidence intervals.

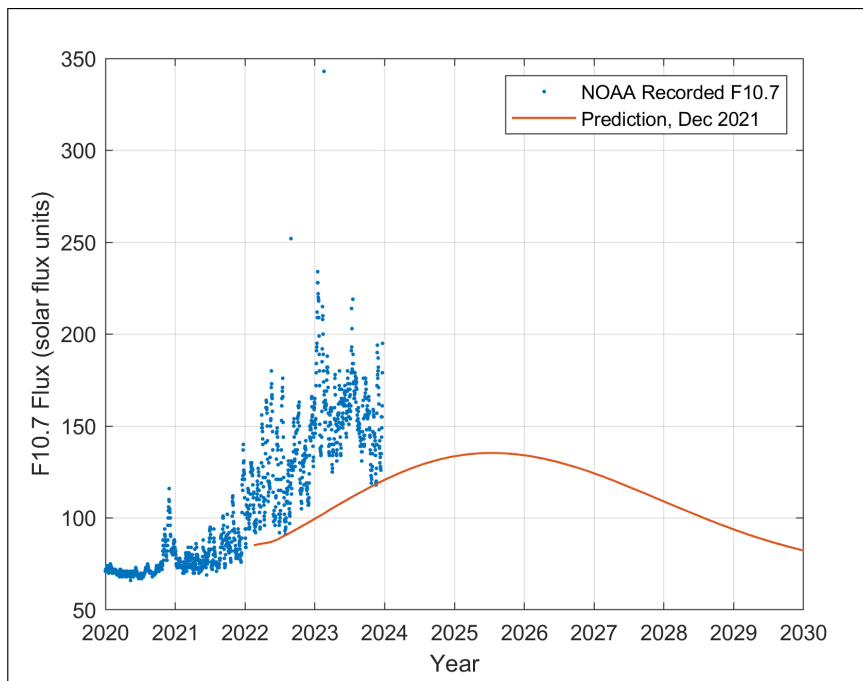


Figure 2. Historical F10.7 solar flux through 20 December 2023 and interpolated NOAA predictions for solar cycle 25 from December 2021.

HUSIR, operated by the Massachusetts Institute of Technology’s Lincoln Laboratory, provides statistical data on orbital debris (OD) down to approximately 5.5 mm up to an altitude of 1000 km and 2 cm to 3 cm throughout low Earth orbit (LEO). The data collected by HUSIR is used to characterize the OD environment in altitude, inclination, and size for a large portion of LEO. Data is collected in a beam park mode, where the antenna is pointed at a fixed azimuth and elevation angle and objects are detected as they pass through the radar beam. Most data are collected using a 75° elevation, due East azimuth (75E) configuration, and data are analyzed on a calendar year (CY) basis. Data from CY 2022 provided the first opportunity for analysis of the Cosmos 1408 breakup fragments over the course of a year.

Comparisons of CY 2022 data to previous years show evidence of increased OD flux at altitudes and inclinations corresponding to Cosmos 1408 at the time of its breakup (ODQN vol. 27, issue 4, October 2023, pp. 3-6). Recently analyzed HUSIR CY 2023 data provides new insights into the state of the fragment cloud 2 full years since the event. Figure 1 shows the flux versus orbit altitude for HUSIR CY 2021, CY 2022, and CY 2023 data, limited to altitudes between 400 km and 1000 km. Detections are limited to Doppler inclinations from 72° to 94°, which showed the highest increase over background levels based on special data collect

continued on page 3

Cosmos 1408

continued from page 2

immediately after the breakup, and debris sizes of 7.2 mm and larger, the 99% completeness limit of HUSIR CY 2022 data. The increased flux from 2021 to 2022 over the 400 km to 500 km altitude range, attributable to the Cosmos 1408 breakup, shows a noticeable drop in 2023 back to levels almost equivalent to those of 2021 within uncertainties. This suggests most of the fragments from the Cosmos 1408 breakup at these altitudes and sizes have decayed out of orbit.

Comparing the current distribution of fragments to modeled predictions shows the Cosmos 1408 fragments have decayed faster than originally modeled. This is attributed to increased solar activity over the past few years; the actual solar flux activity of Solar Cycle 25 has been substantially higher than the original NOAA prediction released in December 2019, prompting NOAA to release an update [1]. Figure 2 shows the observed F10.7 solar flux through 20 December 2023 compared to the solar flux prediction for Solar Cycle 25 from December 2021. The ODPO uses monthly predicted fluxes provided by NOAA, interpolated to daily values, and 27-day NOAA forecasts extending from the end of the observed record to propagate objects into the future (see ODQN vol. 24, issue 4, November 2020, pp. 4-6 for more details). The December 2021 prediction was the most recent prediction available after the Cosmos 1408 ASAT and was used to propagate the Cosmos 1408 debris cloud for updating ORDEM 3.2.

Figures 3 and 4 show the percentage of Cosmos 1408 debris greater than 1 mm and 1 cm, respectively, remaining on orbit as a function of time when propagated using the original December 2021 solar flux prediction (presented in ODQN vol. 26, issue 1, March 2022, pp. 1-5) and the observed historical solar flux through 20 December 2023. The sharp decline in the number of fragments still on orbit over the first few years, as compared to the original predictions, is apparent. After the first 2 years, approximately 7% and 9% of modeled fragments greater than 1 mm and 1 cm, respectively, remain on orbit. This contrasts the approximately 22% and 26% originally estimated using the lower predicted solar flux activity.

Figure 5 shows the number of fragments greater than 7 cm remaining on orbit as a function of time under the two propagation scenarios as well as the orbital decay behavior of cataloged fragments; as of 03 February 2024, the SSN has cataloged 1805 Cosmos 1408 fragments. For cataloged fragments, sizes are converted from publicly available radar cross-section (RCS) to size using the NASA Size Estimation Model. The

7 cm-size limit was observed to provide the best overall match between the cataloged fragments and fragments propagated using the historical solar flux values, in terms of both total number of fragments and general decay behavior.

The cataloged fragments exhibit a lower initial number and slower initial decay rate than the modeled fragments. This is likely

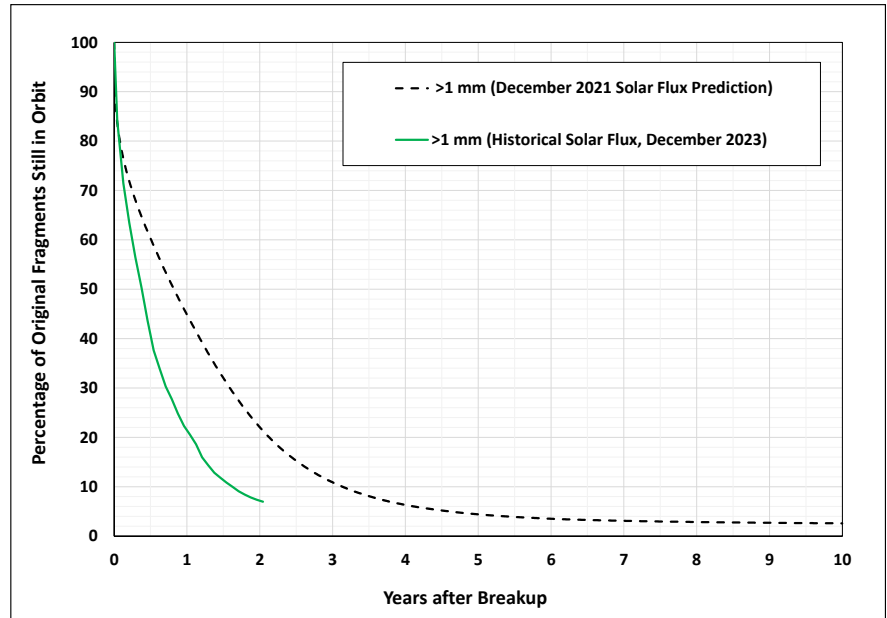


Figure 3. Percentage of Cosmos 1408 fragments 1 mm and larger remaining on orbit as a function of time, propagated using the Solar Cycle 25 prediction from December 2021 (dashed curve) and the historical solar flux through 20 December 2023 (solid curve).

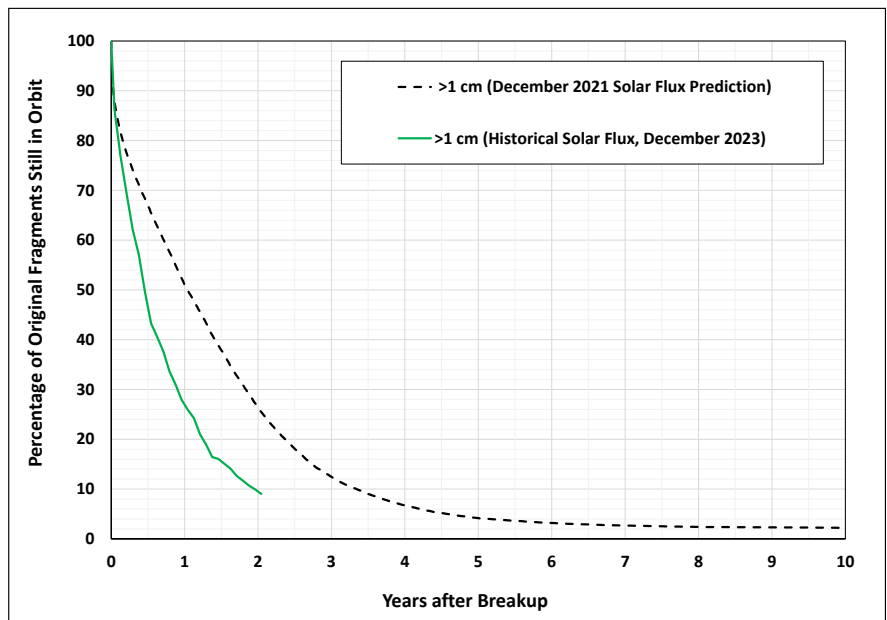


Figure 4. Percentage of Cosmos 1408 fragments 1 cm and larger remaining on orbit as a function of time, propagated using the Solar Cycle 25 prediction from December 2021 (dashed curve) and the historical solar flux through 20 December 2023 (solid curve).

continued on page 4

Cosmos 1408

continued from page 3

because fragments that reentered quickly were not adequately tracked and were thus not cataloged – the first Cosmos 1408

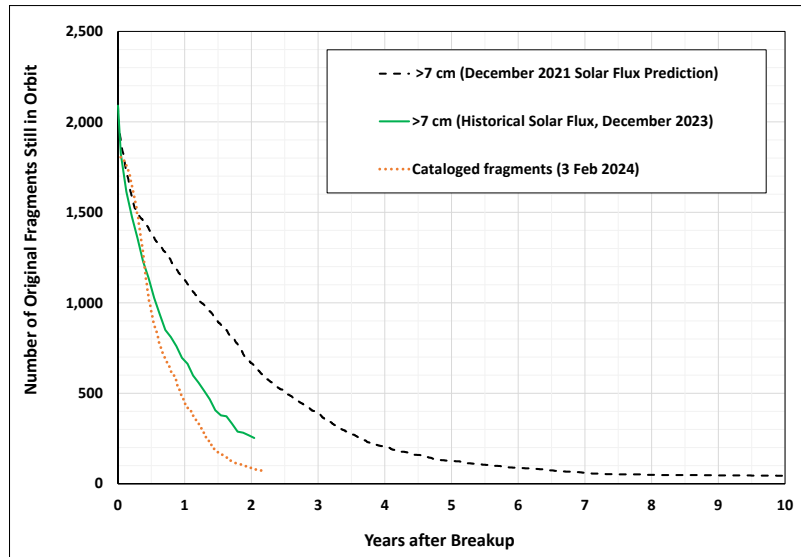


Figure 5. Number of Cosmos 1408 fragments 7 cm and larger remaining on orbit as a function of time, using the Solar Cycle 25 prediction from December 2021 (dashed curve) and the historical solar flux through 20 December 2023 (solid curve). The orbital decay behavior of all cataloged Cosmos 1408 breakup debris, as of 03 February 2024, are shown by the dotted curve.

breakup debris entered the public catalog approximately 2 weeks after the event. Cataloging fragments from new breakups is generally challenging, and many new fragments may reenter before they can be individually detected, tracked, and cataloged. Had more Cosmos 1408 fragments been cataloged in the first few days, it is expected the early part of the cataloged curve would show more similar behavior to the modeled curves.

To capture trends in the orbital evolution of sub-centimeter-sized debris and to provide timely data for validating and updating models of the OD environment, such as ORDEM, it is critical to regularly monitor the OD populations and the space environment, especially solar activity. Comparisons between the modeled Cosmos 1408 breakup and measurement data is ongoing, and the dynamic behavior of the Cosmos 1408 and other debris clouds, based on updated solar cycle predictions, will be incorporated in upcoming ORDEM releases.

Reference

1. “NOAA Forecasts Quicker, Stronger Peak of Solar Activity,” <https://www.swpc.noaa.gov/news/noaa-forecasts-quicker-stronger-peak-solar-activity> [Accessed 14 February 2024]. ♦

Modeling the Small Debris Population in ORDEM – Process Overview

A. KING, P. ANZ-MEADOR, D. VAVRIN, AND M. MATNEY

The NASA Orbital Debris Program Office (ODPO) develops and disseminates models, tools, and utilities to the public to provide a standard, validated means of defining the orbital debris (OD) environment, assessing its risks, and ensuring compliance with relevant policies, practices, and procedures. The Orbital Debris Engineering Model (ORDEM) is a data-driven model; measurements of the environment are used to reconcile initial model-based debris populations with the actual population during the build process, and other independent data sets are used to validate the model. In low Earth orbit (LEO), two data sets are used in the build and validation processes. Radar sensors and networks provide statistical or deterministic measurements of the debris environment down to approximately 3 mm interpreted sizes at altitudes below 1000 km, while *in situ* measurements, via the analysis of returned surfaces, provide data below approximately 1 mm at altitudes below 600 km. This constitutes the small debris population and consists of both degradation by space weathering and ejecta produced by micrometeoroid (MM) and OD impacts.

The small debris population spans the debris size range

of 10 μm to approximately 3 mm, and these particles tend to dominate the debris population in this size range. For model building, the lower size is anchored by *in situ* data collected from the Space Transportation System (STS) window impact data and the upper size by STS radiator perforation data. For model validation, data from the Hubble Space Telescope returned surfaces are used. These measurement data sets provide the means of reconciling a modeled population with the observed population via appropriate scaling of the model population. *In situ* measurements are transformed from impact feature size to debris size using cratering and perforation damage equations defined by ground-based hypervelocity impact testing and hydrocode simulations—an inverse problem. These selfsame damage equations can be used in the forward problem of simulating damage caused by the model environment during build and validation of the model small particle populations. *In situ* data and the damage equations are used consistently in both the inverse and forward methods.

This project review focuses on the methodology used to define an initial small debris population via modeling. An

continued on page 5

ORDEM Modeling

continued from page 4

essential aspect of modeling this population is characterizing the production of small debris – the phenomenology by which small debris are produced by parent objects in orbit. The ODPO has identified two phenomena capable of producing small debris: impacts and surface degradation. First, impacts from either MM or OD create ejecta or spallation that separate from the parent body. Secondly, surface degradation may include effects due to space weathering attributable to thermal stress, the neutral atmosphere, plasma, or ionizing and non-ionizing radiation in addition to the use of space grade or non-space grade surface materials.

The ODPO examined the types of surfaces commonly found on spacecraft and rocket bodies (R/B), including coatings such as paint, solar cells, composite materials, and thermal blankets. Salient findings are that not all surface types are necessarily subject to both specific small debris production phenomena in the size range of interest; a single parent body may feature multiple production surface types; and the long-term influence of production surfaces in near circular and elliptical orbits may differ significantly.

Two distinct methodologies for small particle production modeling have been identified, and these may be termed “first principles modeling” and “statistical modeling.” In the former case parent bodies would be characterized individually or by class according to their surface compositions and composition areas, the sums of which would total the exposed surface area of the object. In the latter case, the known or estimated surface area of these same parent bodies create small debris continuously and are scaled or removed when the model population is reconciled with measurement data. First principles modeling presents multiple technical and non-technical difficulties, for example, determining or defining composition types in the absence of publicly available data; thus, statistical modeling was chosen as offering a tractable path to model the small particle production environment. Once a surface produces small particles, the particles are propagated from their source into the future. In addition to initial orbital parameters, the debris physical parameters of size or characteristic length (L_c), shape, mass density, and area-to-mass ratio, as well as external factors such as historical and predicted solar activity, all serve to influence their orbital evolution. Hence, small debris orbit parameters are categorized into the ORDEM parameter structure on an annual basis and scaled accordingly to measurements as a function of ORDEM orbital parameters and mass density category [1]. Small debris in LEO, LEO-crossing, and geosynchronous (GEO)-crossing orbits are reconciled with measurement data. Debris smaller than 10 cm are not modeled in GEO because there is no corresponding measurement data in that orbital volume to reconcile against the modeled small debris population.

This general approach was used for the development of the ORDEM 3.X series of models, which incorporated debris mass density as an OD environment parameter. The same approach for ORDEM 4.0, currently in development, has been retained but debris shape is added as an additional population parameter

above a threshold size of approximately 316 μm .

With the statistical production model, a small particle population source object of a given month/year is determined using NASA’s long-term environment model, the LEO-to-GEO Environment Debris model LEGEND [2], which provides updated orbital elements of spacecraft and R/Bs as a function of time. The parameters needed to generate new objects for this small particle population are the perigee/apogee altitude, inclination, and final surface area of the parent body at the given production time in question.

The number of small particles generated per given month for a given spacecraft or R/B (known as that particle’s production rate) is determined using a Poisson distribution based on the generic production rate (PR):

$$PR = 0.1 \times SA$$

where surface area in square meters (SA) = CSA*6.0 where CSA represents the cross-sectional area of the parent body if the parent body is a spacecraft. If the parent body is instead a R/B, SA = CSA*4.5 to account for the unique structures associated with R/Bs. The actual production rate is not critical since each small-particle population will be scaled to fit observations. For each small particle generated in this distribution process, a random generation date is determined for that particle within the production year (*i.e.*, PR for a given month within a given year). Then, a random L_c is chosen for that particle within a uniform logarithmic distribution between 10 μm and approximately 3 mm. The L_c determines the shape as well as the length-to-diameter (L:D) ratio – the length L is defined as being equal to the height of the particle, whereas D is akin to the square root of the product of the particle’s major and minor diameters d_1 and d_2 assuming simple elliptical cylinders [3]. The table contains mass densities of high (HD), medium-high (MDHI), medium-low (MDLO), paint (PNT), and fiber-reinforced plastic (FRP), and shape details for nuggets (N), plates (P), or rods (R).

As shown, nuggets tend to be the most likely shape for HD, MDLO, and MDHI with a L:D ratio for these objects

Shape for Various Mass Density Categories for $L_c (\geq 316 \mu\text{m})$

Density		Possible Shape	L:D
Category	Bound (g/cm ³)		
HD	> 6	N	$0.67 < \times < 1.5$
FRP	1.5	P, N, R	Depends on shape
PNT	2.5	P	$\frac{L}{(1.502 \times L_c - 1.034 \times L)}$
MDLO	2 - 4	N	$0.67 < \times < 1.5$
MDHI	4 - 6	N	$0.67 < \times < 1.5$

continued on page 6

ORDEM Modeling

continued from page 5

between 0.67 and 1.5. Due to the production method for FRP, the small particles may resemble either of the three shape categories and are randomly drawn to be either a plate, rod, or nugget based on specific distributions defined for each shape [4]. Paint particles larger than 316 μm are assumed to be plates with a constant thickness of 150 μm , used as L in the L:D equation. Note for particles with $L_c < 316 \mu\text{m}$ that these are automatically considered by the model to be nuggets since a concise definition of their exact shape has not been determined.

After this, a volume (V), SA, and CSA are determined for each particle. Given the table, the L:D ratio for each particle is now known, but L and D must also be calculated individually to determine V:

$$V = \frac{\pi L D^2}{4}, \text{ where } D = \frac{2.7 \times L_c}{\frac{L}{D} + 2} \text{ and } L = \left(\frac{L}{D}\right) \times D$$

$$SA = \pi \left(\frac{L}{D} + 0.5\right) \left(\frac{L_c^2}{\left(\frac{L}{D}\right)^2 + 1}\right)$$

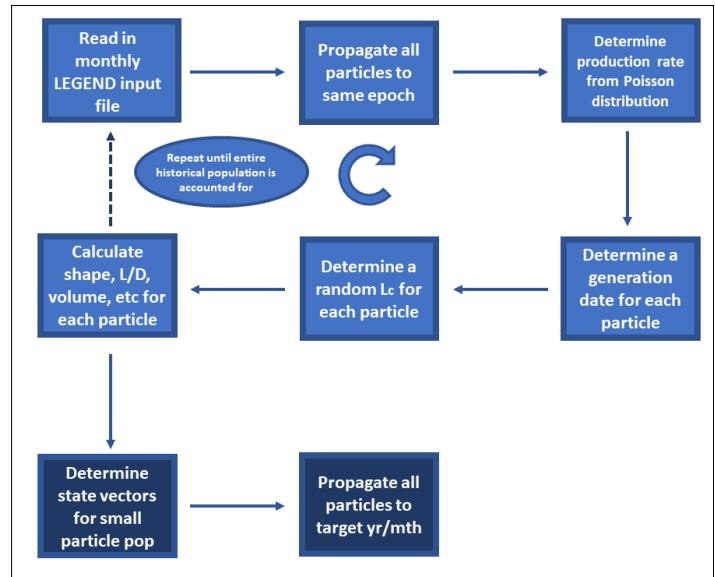
$$CSA = \frac{SA}{4}$$

Finally, using the calculated metrics above in tandem with a given particle's L_c and density ρ , a mass m and area-to-mass A/m for that particle can be determined:

$$m = \rho V$$

$$\frac{A}{m} = \frac{CSA}{m}$$

Once all small particle characteristics are determined, the state vectors that define the velocity of these particles being shed from their parent body are calculated based on the state vector of the parent body at the time of the debris objects "creation." The ODPO propagation tool is used to distribute each of these particles through time in a modeled space environment to the end of a given year/month. Particles that are projected to destructively enter the Earth's atmosphere are removed from the model population during this process, as shown in the figure. The next step in the build process is to apply fits to the model to reconcile it with *in situ* measurements.



The Statistical Production Modeling process flow.

Statistical production models for the initial small particle model environment have demonstrated their flexibility and utility in prior versions of ORDEM. The development of ORDEM 4.0, incorporating debris shape parameters for the first time, provides yet another opportunity to improve the overall development of accurate computer models of the small particle OD environment.

References

1. Seago, J., *et al.* "Development of a Model for the Small-Particle Orbital Debris Population Based on the STS Impact Record," First International Orbital Debris Conference, (2019), <https://www.hou.usra.edu/meetings/orbitaldebris2019/pdf/6137.pdf> (accessed February 2024).
2. Liou, J.-C., *et al.* LEGEND – "A three-dimensional LEO-to-GEO debris evolutionary model," *Adv. Space Res.* 34, 5, pp. 981-986, (2004).
3. Seago, J., *et al.* "An Approach to Shape Parameterization Using Laboratory Hypervelocity Impact Experiments," Second International Orbital Debris Conference, (2023), <https://www.hou.usra.edu/meetings/orbitaldebris2023/pdf/6145.pdf> (accessed February 2024).
4. Cowardin, H., *et al.* "Updates on the DebrisSat Hypervelocity Experiment and Characterization of Fragments in Support of Environmental Models," *International Journal of Impact Engineering*, Volume 180, October 2023, 104669, <https://doi.org/10.1016/j.ijimpeng.2023.104669> . ♦

MEETING REPORT

The NASA-DOD Orbital Debris Working Group Meeting, 28 November 2023, Virtual

The 26th annual NASA-DOD Orbital Debris Working Group meeting was held virtually on 28 November 2023. This annual, one-day meeting provides a framework for cooperation and collaboration between NASA and the DOD on orbital debris-related activities, such as measurements, modeling, mitigation, and policy development. NASA and the DOD have benefited significantly from this group, and many collaborations directly result from this working group. This year's meeting was co-chaired by the NASA Orbital Debris Program Office (ODPO) and by the Operational Assessments Division, HQ Space Operations Command, U.S. Space Force (USSF).

After opening remarks, NASA began with a presentation on the U.S. Government Orbital Debris Mitigation Standard Practices, followed by an update on the next-generation Orbital Debris Engineering Model, ORDEM 4.0. The ODPO then gave an update on the DebrisSat project and the fusion of measurements and analysis from the project into ORDEM 4.0 and the NASA Standard Satellite Breakup Model.

Two ODPO presentations on radar and optical measurement activities were presented: first, the low Earth orbit debris

environment as revealed by recent measurements from the Haystack Ultrawideband Satellite Imaging Radar (HUSIR) and the Goldstone Orbital Debris Radar; then, an update on the Eugene Stansbery - Meter Class Autonomous Telescope (ES-MCAT). The ES-MCAT recently completed a re-coating of the primary mirror and began its second survey of the geosynchronous region in January 2023 (ODQN, vol. 27, issue 1, March 2023, pp. 4-5). The final ODPO presentation included updates on reentry analysis activities, including inspection of a recovered fragment of the Dragon 2 trunk that reentered over Australia in July 2022.

The DOD personnel with the 18th Space Defense Squadron at Vandenberg Space Force Base presented an overview of the on-orbit breakup detection and analysis process. This was followed by an update on the Space Surveillance Telescope as it proceeded through initial operating capability to operational acceptance into the Space Surveillance Network in September 2022. Next, the USSF summarized the flow of observation data for uncorrelated tracks for the Space Fence. The final DOD presentation discussed research and other efforts toward debris mitigation in cislunar space. ♦

UPCOMING MEETINGS

13-21 July 2024: Committee on Space Research (COSPAR) 2024, BEXCO, Busan, Korea

The 45th Assembly of the Committee on Space Research (COSPAR) Scientific Assembly will convene in the Busan Exhibition and Convention Center, BEXCO. The COSPAR panel on Potentially Environmentally Detrimental Activities in Space (PEDAS) will conduct a program entitled "A Sustainable Space Exploration: from the Mitigation of Space Debris in Earth's Orbit to the Safeguard of Planetary Environments." The main topics to be discussed in the PEDAS.1 sessions will include orbital debris observations and measurements; environmental models and databases; modeling and risk analysis; mitigation and remediation; sustainable space activities; national and international standards and guidelines; mega-constellation impact on astronomy; pollution of the Earth's atmosphere by rocket launches and re-entries; cis-lunar space; and Lunar and Martian environments. The abstract submission period closed on 09 February 2024. Please see the PEDAS.1 session website at https://www.cospar-assembly.org/admin/session_cospar.php?session=1295 and the Assembly website at: <https://www.cospar2024.org/>.

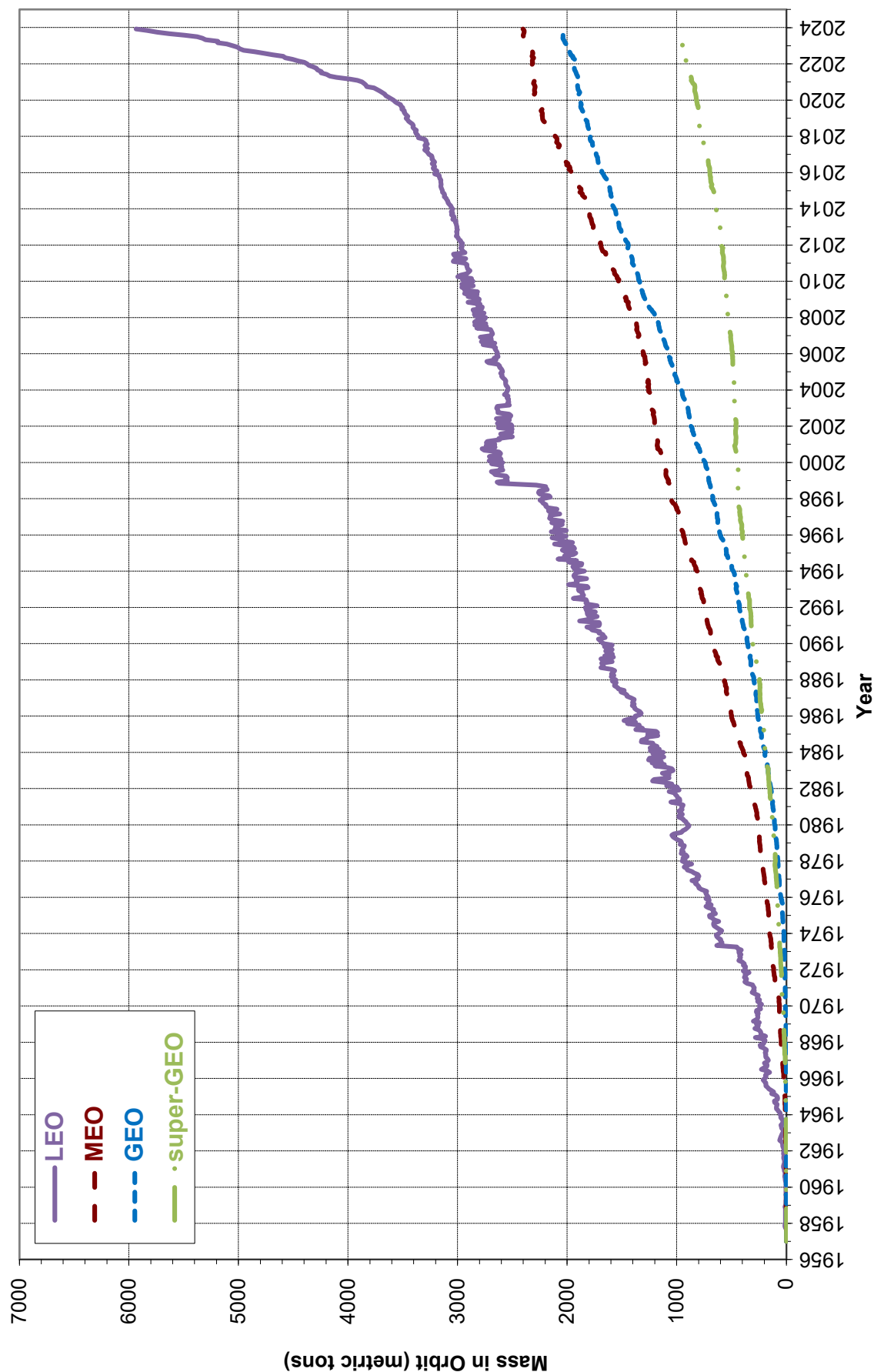
14-18 October 2024: 74th International Astronautical Congress (IAC), Milan, Italy

The IAC will convene in 2024 with a theme of "Responsible Space for Sustainability." The IAC's 22nd IAA Symposium on Space Debris will cover space debris detection, tracking and characterization; modeling; risk analysis; hypervelocity impact and risk assessments; mitigation; post-mission disposal and space debris removal; operations in the space debris environment; political, legal, institutional, and economics aspects of mitigation and removal; and orbit determination and propagation. Interactive presentations on space debris topics will also be provided to allow more digital display capabilities for attendees. The abstract submission period closed on 28 February 2024. Additional information for the 2024 IAC is available at <https://www.iafastro.org/events/iac/international-astronautical-congress-2024/> and <https://www.iac2024.org/>.

17-20 September 2024: 25th Advanced Maui Optical and Space Surveillance Technologies Conference (AMOS), Maui, Hawaii, USA

The technical program of the 25th Advanced Maui Optical and Space Surveillance Technologies Conference (AMOS) will focus on subjects that are mission critical to space situational awareness. The technical sessions include papers and posters on space debris; space situational/space domain awareness (SDA); SDA systems and instrumentation; astrodynamics; satellite characterization; space weather; and related topics. The abstract submission deadline was 01 March 2024. Registration for this hybrid conference opens in April 2024 for in-person and virtual attendees. Additional information about the conference is available at <https://amostech.com>. ♦

Monthly Effective Mass of Objects in Earth Orbit



Monthly Effective Mass of Objects in Earth Orbit by Orbital Regime cataloged by the U.S. Space Surveillance Network. This chart displays the mass of all objects in Earth orbit officially cataloged by the U.S. Space Surveillance Network. Low Earth orbit (LEO) includes resident space objects (RSOs) with altitudes within or crossing below 2000 km; medium Earth orbit (MEO) RSOs with altitudes within or crossing the range from 2000 km to 35,586 km; geosynchronous orbit (GEO) RSOs with altitudes within or crossing the range from 35,586 km to 35,986 km; and the remainder with altitudes within or crossing the range from 35,986 km to 600,000 km, referred to as Super-GEO. "Effective" mass scales the mass of each object by the fraction of its orbit that falls within the specified altitude ranges. Cataloged objects without available orbital elements are excluded.

Debris Assessment Software 3.2.6 Release

The NASA Orbital Debris Program Office has released version 3.2.6 of the Debris Assessment Software (DAS), replacing the prior June 2023 release of DAS 3.2.5. The updated version provides data that can verify compliance of a spacecraft, upper stage, and/or payload with NASA’s requirements for limiting debris generation, spacecraft vulnerability, post-mission disposal, and reentry safety.

This release incorporates a fix to the cross-sectional area tool, where some shapes were not correctly read in before processing. The apogee-perigee history tool also received a fix for apparent fast reentries from high altitudes; this issue was localized to the science utility and did not affect requirement verification. Finally, a fix was implemented for Requirement 4.5-2, small particle penetration assessment, where some layers were not read in correctly before processing.

Users who have already completed the software request process for earlier versions of DAS 3.x do not need to reapply for DAS 3.2.6. Simply go to your existing account on the NASA Software portal and download the latest installer. Due to file size limits, the installer has been split into several .zip archive files: the main installer and five separate files containing debris environment data. Users must download the main installer (which includes the debris environment for years 2016 to 2030) and additional environment files required to assess mission years beyond 2030.

Approval for DAS is on a per project basis; approval encompasses activities and personnel working within the project scope identified in the application. For new users, DAS is available for download, pending an approved application submission, via the NASA Software Catalog. To begin the process, click on the Request Software button at <https://software.nasa.gov/software/MSC-26690-1>.

INTERNATIONAL SPACE MISSIONS 01 November 2023 – 31 January 2024

Intl.* Designator	Spacecraft	Country/ Organization	Perigee Alt. (KM)	Apogee Alt.(KM)	Incli. (DEG)	Addnl. SC	Earth Orbital R/B	Other Cat. Debris
1998-067	ISS dispensed objects	Various	415	423	51.6	2	0	1
2023-169A	TJS-10	PRC	35757	35818	0.4	0	1	0
2023-170A	STARLINK-30800	US	558	560	43.0	22	0	0
2023-171A	STARLINK-30861	US	553	554	43.0	22	0	0
2023-172A	CHINASAT-6E	PRC	35783	35789	0.0	0	1	0
2023-173A	DRAGON CRS-29	US	232	401	51.6	0	0	1
2023-174A	CONNECTA T3.1	TURK	513	525	97.5	104	0	0
2023-175A	O3B MPOWER F05	SES	6186	8230	2.1	0	1	0
2023-175B	O3B MPOWER F06	SES	6328	8248	3.1			
2023-176A	HAIYANG 3A	PRC	767	789	98.6	0	1	0
2023-177A	STARLINK-30901	US	299	305	43.0	22	0	0

continued on page 10

SATELLITE BOX SCORE

(as of 04 March 2024, cataloged by the U.S. SPACE SURVEILLANCE NETWORK)

Country/ Organization	Spacecraft*	Spent Rocket Bodies & Other Cataloged Debris	Total
CHINA	674	4330	5004
CIS	1568	5529	7097
ESA	96	28	124
FRANCE	88	533	621
INDIA	110	101	211
JAPAN	208	111	319
UK	701	1	702
USA	7590	5011	12601
OTHER	1180	83	1263
Total	12215	15727	27942

* active and defunct

Visit the NASA

Orbital Debris Program Office Website

www.orbitaldebris.jsc.nasa.gov

Technical Editor

Heather Cowardin, Ph.D.

Managing Editor

Ashley Johnson

Correspondence can be sent to:

Robert Margetta

robert.j.margetta@nasa.gov

or to:

Nilufar Ramji

nilufar.ramji@nasa.gov

National Aeronautics and Space Administration

Lyndon B. Johnson Space Center

2101 NASA Parkway

Houston, TX 77058

www.nasa.gov

<https://orbitaldebris.jsc.nasa.gov/>



INTERNATIONAL SPACE MISSIONS

01 November 2023 – 31 January 2024

Intl.* Designator	Spacecraft	Country/ Organization	Perigee Alt. (KM)	Apogee Alt.(KM)	Incli. (DEG)	Addnl. SC	Earth Orbital R/B	Other Cat. Debris
2023-178A	STARLINK-30911	US	509	511	53.1	21	0	0
2023-179A	MALLIGYONG-1	NKOR	497	508	97.4	0	1	0
2023-180A	STARLINK-30964	US	556	557	43.0	22	0	0
2023-181A	OBJECT A	PRC	1094	1114	50.0	2	0	0
2023-182A	COSMOS 2572	CIS	294	305	96.7	0	1	0
2023-183A	STARLINK-30869	US	558	560	43.0	22	0	0
2023-184A	PROGRESS MS-25	CIS	415	423	51.6	0	1	0
2023-185B	KORSAT 7	SKOR	552	570	97.6	17	0	0
2023-186A	STARLINK-30947	US	558	560	43.0	22	0	0
2023-187B	MISRAT-2	EGYP	625	643	98.0	2	0	1
2023-188A	DOORY-SAT	SKOR	637	650	47.0	0	1	0
2023-189A	OBJECT A	PRC	491	511	97.5	0	1	0
2023-189B	OBJECT B	PRC	487	507	97.5	0	1	0
2023-190A	OBJECT A	PRC	909	926	86.5	0	0	2
2023-191A	STARLINK-31026	US	488	488	43.0	22	0	0
2023-192A	STARLINK-31012	US	481	482	53.2	21	0	0
2023-193A	OBJECT A	PRC	425	453	97.3	0	0	1
2023-193B	OBJECT B	PRC	454	465	97.3	0	0	0
2023-193C	OBJECT C	PRC	459	499	97.3	0	0	0
2023-194A	OBJECT A	PRC	490	503	35.0	0	1	1
2023-194B	OBJECT B	PRC	496	499	35.0	0	0	0
2023-194C	OBJECT C	PRC	493	500	35.0	0	0	0
2023-195A	PRC TEST SPACECRAFT 3	PRC	602	609	50.0	0	1	4
2023-196A	QPS-SAR-5 TSUKUYOMI-H	JPN	571	578	42.0	0	2	0
2023-197A	YAOGAN-41	PRC	35727	35848	4.8	0	1	0
2023-198A	OBJECT A	CIS	1474	38882	63.3	0	0	0
2023-198B	OBJECT B	CIS	1424	39206	63.3	0	0	0
2023-199A	OBJECT A	PRC	484	499	97.4	0	0	0
2023-199B	OBJECT B	PRC	249	399	97.7	0	0	0
2023-199C	OBJECT C	PRC	123	167	97.7	0	0	0
2023-200A	STARLINK-31044	US	487	489	43.0	22	0	0
2023-201A	COSMOS 2573	CIS	491	510	97.6	0	1	0
2023-202A	TYVAK-1015 (TANTRUM)	US	131	163	140.0	0	1	0
2023-203A	STARLINK-31119	US	187	213	43.0	22	0	0
2023-204A	SRH2	GER	NO ELEMS. AVAILABLE		0	0	0	0
2023-204B	SRH1	GER	NO ELEMS. AVAILABLE		0	0	0	0
2023-205A	TIANMU-1 11	PRC	514	532	97.4	3	1	0
2023-206A	SHIYAN 24C 01	PRC	536	555	97.3	2	1	0
2023-207A	BEIDOU-3 M25	PRC	21515	21541	55.0	0	2	0
2023-207B	BEIDOU-3 M26	PRC	21512	21544	55.0	0	0	0
2023-208A	TIANMU-1 19	PRC	517	533	97.4	3	1	0
2023-209A	COSMOS 2574	CIS	334	345	96.8	0	1	1
2023-210A	USA 349	US	NO ELEMS. AVAILABLE		0	0	0	0
2023-211A	STARLINK-31130	US	185	191	43.0	22	0	0
2023-212A	HJS-4A	PRC	933	945	50.0	2	0	0
2024-001A	XPOSAT	IND	638	653	6.0	0	1	0
2024-002A	STARLINK-11072	US	359	360	53.2	20	0	0
2024-003A	OVZON-3	SWED	EN ROUTE TO GEO		0	1	0	0
2024-004A	TIANMU-1 15	PRC	517	533	97.5	3	1	0
2024-005A	STARLINK-31155	US	491	495	43.0	22	0	0
2024-006A	PEREGRINE	US	REENTRY FROM LUNAR TRANS.		0	0	0	0
2024-007A	EINSTEIN PROBE	PRC	579	595	29.0	0	1	0
2024-008A	TIANXING-1 02	PRC	314	317	95.1	0	1	0
2024-009A	YUNYAO-1 18	PRC	471	489	50.0	2	1	0
2024-010A	IGS O-8	JPN	NO ELEMS. AVAILABLE		0	1	1	1
2024-011A	STARLINK-31127	US	548	550	53.2	21	0	0
2024-012A	STARLINK-31189	US	488	488	43.0	22	0	0
2024-013A	TIANZHOU 7	PRC	375	386	41.5	0	1	2
2023-063C	DALIAN-1 LIANLI	PRC	331	351	41.5	0	0	0
2024-014A	AXIOM-3	US	212	400	51.6	0	0	1
2024-015A	SORAYA	IRAN	744	760	64.5	0	1	1
2024-016A	OBJECT A	PRC	519	540	97.5	0	0	0
2024-016B	OBJECT B	PRC	520	541	97.5	0	0	0
2024-016C	OBJECT C	PRC	520	541	97.5	0	0	0
2024-016D	OBJECT D	PRC	520	541	97.5	0	0	0
2024-016E	OBJECT E	PRC	279	517	97.7	0	0	0
2024-016F	OBJECT F	PRC	520	540	97.5	0	0	0
2024-017A	STARLINK-31233	US	480	483	53.2	21	0	0
2024-018A	OBJECT A	IRAN	456	1108	58.7	0	0	0
2024-018B	OBJECT B	IRAN	456	1103	58.7	0	0	0
2024-018C	OBJECT C	IRAN	457	1099	58.7	0	0	0
2024-018D	OBJECT D	IRAN	456	1099	58.7	0	0	0
2024-019A	STARLINK-31238	US	430	431	43.0	22	0	0
2024-020A	STARLINK-31306	US	481	483	53.2	21	0	0
2024-021A	CYGNUS NG-20	US	415	423	51.6	0	0	0
2021-102N	DRUMS TARGET-2	JPN	527	552	97.5	0	0	0
2024-022A	LEMUR 2 NIMBUS2000	US	519	540	97.5	3	2	0

Intl. = International; SC = Spacecraft; Alt. = Altitude; Incli. = Inclination; Addnl. = Additional; R/B = Rocket Bodies; Cat. = Cataloged

Notes: 1. Orbital elements are as of data cut-off date 31 January. 2. Additional spacecraft on a single launch may have different orbital elements. 3. Additional uncatalogued objects may be associated with a single launch.